Surface-Plasmon-Coupled Emission of Quantum Dots

Ignacy Gryczynski,[†] Joanna Malicka,[†] Wen Jiang,[‡] Hans Fischer,[‡,§] Warren C. W. Chan,[‡,§] Zygmunt Gryczynski,[†] Wojciech Grudzinski,[†] and Joseph R. Lakowicz*[,†]

Center for Fluorescence Spectroscopy, Department of Biochemistry and Molecular Biology, University of Maryland School of Medicine, 725 West Lombard Street, Baltimore, Maryland 21201, and Institute of Biomaterials and Biomedical Engineering and Department of Materials Science & Engineering, University of Toronto, Rosebrugh Building 407 and 421, 4 Taddle Creek Road, Toronto, ON, M5S 3G9 Canada

Received: August 24, 2004; In Final Form: October 26, 2004

We studied surface plasmon-coupled emission (SPCE) of semiconductor quantum dots (QDs). These QDs are water-soluble ZnS-capped CdSe nanoparticles stabilized using lysine cross-linked mercaptoundecanoic acid. The QDs were spin-coated from 0.75% PVA solution on a glass slide covered with 50 nm of silver and a 5-nm protective SiO_2 layer. Excited QDs induced surface plasmons in a thin silver layer. Surface plasmons emitted a hollow cone of radiation into an attached hemispherical glass prism at a narrow angle of 48.5°. This directional radiation (SPCE) preserves the spectral properties of QD emission and is highly p-polarized irrespective of the excitation polarization. The SPCE spectrum depends on the observation angle because of the intrinsic dispersive properties of SPCE phenomenon. The remarkable photostability can make QDs superior to organic fluorophores when long exposure to the intense excitation is needed. The nanosize QDs also introduce a roughness near the metal layer, which results in a many-fold increase of the coupling of the incident light to the surface plasmons. This scattered incident illumination transformed into directional, polarized radiation can be used simultaneously with SPCE to develop devices based on both quantum dot emission and light scattered from surface plasmons on a rough surface.

Introduction

Fundamental research in the field of nanotechnology is expected to provide new insights into the design of a new generation of biosensors, light-emitting diodes, and computer chips. The potential impact of these nanoscale devices could be immense, and because of this, the field of nanotechnology has garnered tremendous attention from researchers from diverse research backgrounds. New synthetic strategies have been developed for designing and tuning the optical and electronic properties of nanostructures (e.g., metallic, semiconductor, and organic nanoparticles).[1−5] The utilization of these nanostructures for real-world applications has already been demonstrated.[6−11] Examples include the use of metallic and semiconductor nanostructures for biobarcodes and optical probes. A key challenge in the field of nanotechnology is the ability to assemble nanostructures into functional devices; this assembled system will ideally take advantage of the unique properties of the nanostructures. With a plethora of synthetic nanostructures available, studies on the optical and electronic properties of nanostructure interactions are somewhat lacking, and without these studies, there are no guarantees that the properties of the nanostructures are preserved in the assembled systems. In this paper, we studied the interactions of nanometer-thick metallic film and semiconductor nanostructures assembled on a surface. Specifically, we are focused on the surface-plasmon-coupled emission of metallic/semiconductor heterostructures.

Nanometer-sized noble-metal layers or nanoparticles are known to display dramatically reduced reflectance at specific angles during optical excitation. This reduction in the reflectance is due to the excitation of the plasmon on the surface of the metal layer or nanoparticle, a process called surface plasmon resonance.[12−14] The binding of macromolecules on the surface of the metal film or nanoparticle can generate shifts in the reflectivity by altering the surface reflective index and thickness.[15−20] Recently, we described a phenomenon, similar to surface plasmon resonance, called surface plasmon-coupled emission (SPCE).[21−25] In SPCE, we observed interesting optical properties of light reflectivity when fluorophores were coupled to the surface plasmon of a thin metal film. The fluorescence emission was found to be identical to that of the fluorophore, except that it was highly p-polarized and had directional emission. We concluded that the p-polarization and angular dependence of the SPCE are consistent with radiating plasmon, i.e., the reverse process of surface plasmon absorption. On the basis of these fundamental studies, we have developed SPCE for genomic and proteomic applications.[23,24] However, all of these studies have focused on the SPCE of fluorescent organic dye molecules on thin metal films.

Semiconductor quantum dots (QDs) have been introduced as an alternative to organic fluorescent tags for optical imaging and spectroscopy.[9,10,26−28] QDs are nanometer-sized inorganic structures with physical dimensions smaller than the exciton Bohr radius. QDs exhibit unique light emission by changing size or composition, and because of this, they have been exploited for a broad-range of applications. Currently, there are no published reports on the SPCE of QDs. We aim to address two important issues: (1) how the surface plasmon of nanometer-sized metallic surfaces influences the optical emission

* Corresponding author. Tel.: 410 706 8409. Fax: 410 706 8408. E-mail: lakowicz@cfs.umbi.umd.edu.
[†] University of Maryland School of Medicine.
[‡] Institute of Biomaterials and Biomedical Engineering, University of Toronto.
[§] Department of Materials Science & Engineering, University of Toronto.

10.1021/jp046173i CCC: $30.25
Published on Web 12/31/2004

of QDs and (2) how metallic film−QD heterostructures affect the reflectivity of the excitation beam. Our findings in these areas can lead to the design of better optical probes for bioimaging, devices for drug discovery or high-throughput drug screening, optics for the telecommunication and microscopy, or nanoscale electronics.

Materials and Methods

Synthesis and Preparation of Quantum Dots. ZnS-capped CdSe QDs were synthesized using an organometallic approach[5] and water-solubilized and stabilized using lysine cross-linked mercaptoundecanoic acid.[29] Briefly, CdSe QDs were synthesized by rapid injection of precursor $Cd(CH_3)_2$/Se solution into tri-*n*-octylphosphine oxide (TOPO, Aldrich) at 350 °C and grown at 300 °C. After the QDs had reached the desired size, the temperature was lowered to 270 °C, and $Zn(CH_3)_2$ and trimethoxysilosilane were slowly dripped into the reaction vessel. The temperature was then lowered to 70 °C, and the QDs were precipitated out with methanol (Aldrich). These QDs were coated with TOPO and were insoluble in aqueous solvent. To modify the surface of the QDs, the TOPO molecule was exchanged with mercaptoundecanoic acid (MUA, Aldrich), and the surface MUA layer was cross-linked with lysine and dicyclohexylcarbodiimide (Aldrich) in DMSO (Aldrich) and purified using dialysis. The relative quantum yield of the QDs was determined by comparison with the organic dye molecule rhodamine 6G. We characterized the QDs using fluorescence, UV spectrophotometry, and transmission electron microscopy.

Sample Preparation. Glass slides were coated by vapor deposition by EMF Corp. (Ithaca, NY). A 50-nm-thick layer of silver was deposited on the glass followed by a 5-nm-thick SiO_2 protective layer. QDs were deposited on the surface by spin coating at 3000 rpm with a 0.75% solution of poly(vinyl alcohol) (PVA, MW 13000−23000; Aldrich). The optical density of the QD/PVA solution was about 0.005 at 465 nm. The reference slide for the control experiment was prepared from an identical 0.75% PVA solution without QDs. The thickness of the sample was determined by comparison of the measured SPCE angle with the calculated reflectance for the emission wavelength (585 nm).

Reflectance Calculations. The angular distribution of radiated light in the glass prism was determined by the same wavevector matching requirements as for surface plasmon resonance (SPR). For this reason, the equations used in SPR theory can be applied to describe the angular distribution of SPCE using the emission wavelength. In this work, the reflectance profiles of the thin film were calculated using TFCalc 3.5 software (Software Spectra Inc., Portland, OR).

Fluorescence Measurements. Excitation, emission, and anisotropy spectra in solution were measured in a square geometry using an SLM8000 spectrofluorometer equipped with a xenon lamp.

Time-domain lifetime measurements were carried out using a compact fluorescence lifetime spectrometer (FluoTime 100, PicoQuanT GmbH, Berlin, Germany). Excitation pulses (440 nm, 10 MHz, 60 ps in width) came from a laser diode system (PTD 800B with LDH PC 440, PicoQuanT GmbH). To avoid scattered light a cutoff filter (500 nm) was used in the emission channel. All measurements were done using magic-angle conditions. Data analysis was performed using multiexponential fluorescence decay fitting software FluoroFit ver. 3.2.0 (PicoQuanT GmbH).

For SPCE measurements, the spin-coated slides were attached to a hemispherical prism made of BK7 glass using nonfluorescent index-matching fluid (SL-5262, Santolight JV, MO). This combined sample was positioned on a precise rotary stage, which allows excitation and observation at any desired angle relative to the vertical axis around the cylinder.[22] For excitation, we used the reverse Kretschmann (RK) configuration (Figure 1). Observation of the angular distribution of the emission was performed with a 3-mm-diameter fiber, covered with a 500-μm vertical slit, positioned about 15 cm from the sample. This corresponds to an acceptance angle below 0.2°. The output of the fiber was directed toward an SLM8000 spectrofluorometer. For excitation, we used 514-nm illumination from an argon ion laser. A holographic 514.5 supernotch-plus filter (Kaiser Optical System, Inc., Ann Arbor, MI) was used to suppress excitation in the QD SPCE measurements.

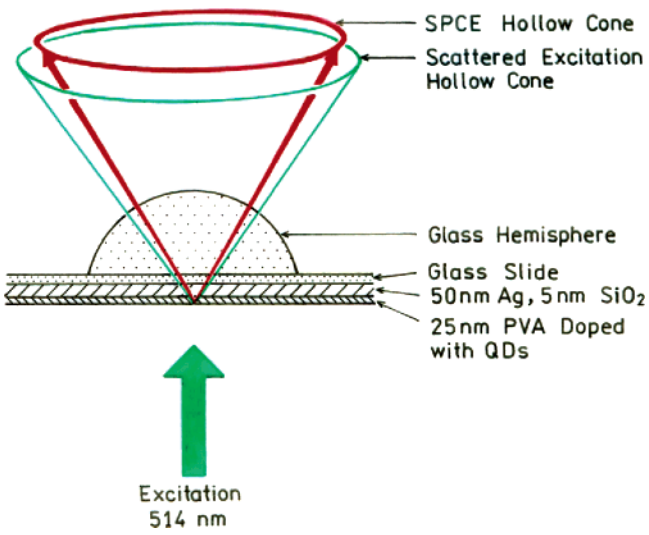

Figure 1. Sample assembly for QD SPCE measurements. The glass slide with the sample was attached to the hemispherical glass prism using an index-matching fluid. Two cones of directional radiation enter the coupling prism at slightly different angles. The QD's orange SPCE radiates inside a narrow green cone of directional scattered excitation.

Results and Discussion

Characterization of QDs. In all experiments, water-soluble ZnS-capped CdSe QDs with a maximum fluorescence emission of 585 nm were used. These QDs were synthesized using an organometallic procedure.[5] Their surface initially contained the surfactant molecule tri-*n*-octylphosphine oxide (TOPO), but the surface was modified with the bifunctional molecule mercaptoundecanoic acid (MUA) to render the QDs compatible with the spin-coating polymer. The MUA was stabilized against desorption from the surface by cross-linking with lysine. Optical and transmission electron microscopy (TEM) imaging revealed the QDs to be monodisperse when dissolved in distilled water. Figure 2 shows the dark-field TEM image of these QDs. Furthermore, the TEM image revealed these QDs to be spherical with a measured aspect ratio of ∼1:1. Anisotropy measurements confirmed the spherical shape of the QDs; the anisotropy value did not exceed 0.07. Hence, the QDs for all experiments had a MUA−lysine cross-linked surface for stabilization, a thin-layer of ZnS (∼1 nm), and a CdSe core (∼4.5 nm).

We measured the optical properties of these QDs (Figure 3). Their absorbance profile was found to be continuous, and the quantum confinement peak was measured at 460 nm. The bulk fluorescence profile was narrower than those of most organic dye molecules [full-width at half-maximum (fwhm) ≈ 40 nm]. We concluded from the fwhm measurements and TEM images

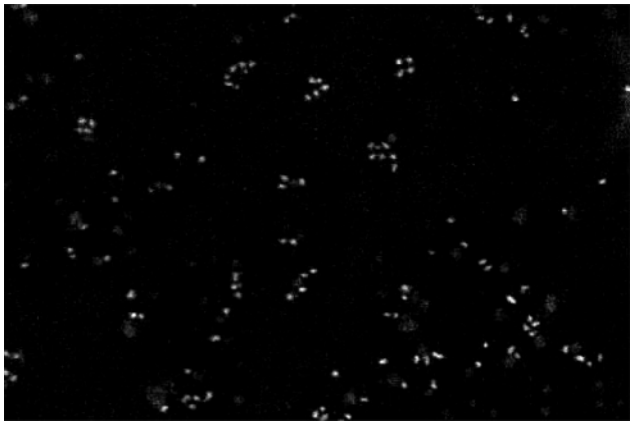

Figure 2. Dark-field TEM image of water-soluble ZnS-capped CdSe quantum dots dispersed in distilled water. Each quantum dot is ~5.5 nm in diameter and the measured aspect ratio is ~1:1. The TEM system is a Hitachi HD-2000, the applied voltage is 200 kV, and the magnification is 100 000×.

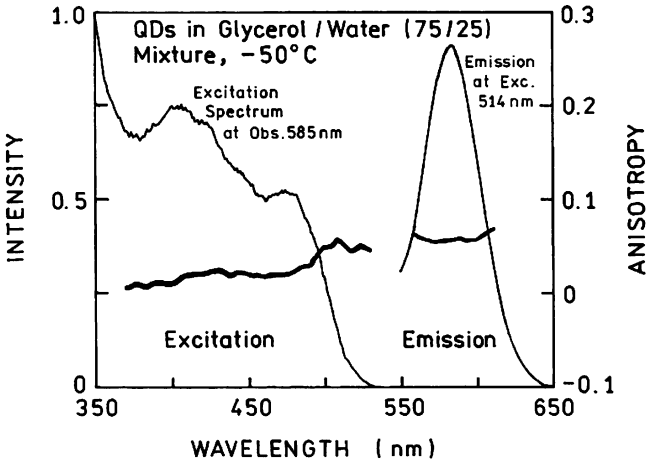

Figure 3. Excitation and emission spectra of QDs in a glycerol/water (75:25, v/v) mixture at −50 °C. Also shown are excitation and emission anisotropy spectra of QDs. The low values of observed anisotropies indicate a dominantly spherical shape of the QDs.

that the QDs had a narrow size distribution (~5% coefficient of variation). In comparison to the organic dye molecule rhodamine 6G, we estimated the relative quantum yield to be ~13−20%. The fluorescence lifetime of these QDs was ~17.1 ns with a heterogeneous intensity decay curve (see Figure 4). The curve fit a four-exponential decay model with lifetimes of 0.38, 2.75, 11.3, and 44.4 ns.

Design of SPCE Assembly and Measurement System. The system to measure the SPCE phenomenon of QDs is shown in Figure 1, where the substrate of Ag, SiO_2, QDs, and glass hemisphere are assembled in a specific order and geometry. In the preparation process, Ag was initially deposited onto a glass surface with refractive index $n_g = 1.52$, followed by a thin layer of the SiO_2 ($n_p = 1.48$). The dielectric constants of silver at 514 and 585 nm are $\epsilon_{Ag}^{514} = -9.0 + 0.31i$ and $\epsilon_{Ag}^{585} = -13.1 + 0.35i$, respectively (TFCalc 3.5 software, Software Spectra Inc., Portland, OR). The SiO_2 layer is a spacer between the QDs and the metal surface; recent reports showed that quenching or enhancing of fluorescence by metal surfaces is distance-dependent.[22] The thin-layer spacer ensured that the fluorescence of the QDs was not quenched by the metal surface. Finally, a thin-layer of QDs, dissolved in 0.75% poly(vinyl alcohol) (PVA, $n_s = 1.50$), was deposited on top of the SiO_2. The thicknesses of the different layers were 50 nm for the Ag layer, 5 nm for the SiO_2 layer, and 25 nm for the QD-doped PVA layer.

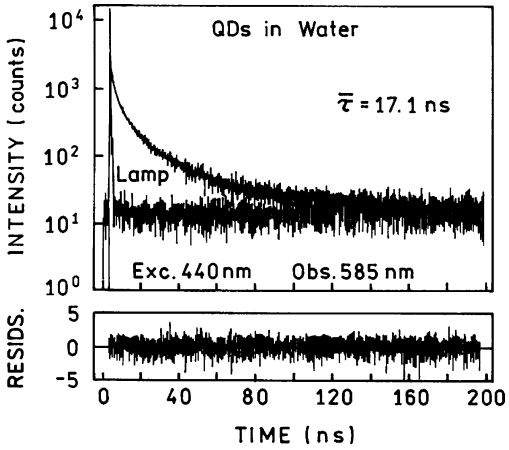

Figure 4. Emission intensity decay of quantum dots dispersed in distilled water at 20°. The decay is heterogeneous and can be satisfactorily fitted to a four-exponential model with lifetimes of 0.38, 2.75, 11.3, and 44.4 ns and relative amplitudes of 0.575, 0.297, 0.109, and 0.019, respectively. The relative mean lifetime is 17.1 ns.

For SPCE studies, the incident light beam of 514 nm excited the sample assembly from the QD side. The hemispherical glass prism (with index matching fluid) on the Ag side was used to collect the emission and scattering from the induced surface plasmons. We observed two effects: (1) directional orange surface-plasmon-coupled emission of QDs and (2) surface plasmon induction on thin Ag layer by the scattered green (514 nm) illuminating source. The plasmons emit to the coupling hemispherical prism in the form of hollow cones, with the green cone outside. This excitation/emission setup is called the reverse Kretschmann (RK) configuration. In the RK configuration, the incident light does not directly excite the surface plasmons. We selected the RK configuration instead of the Kretschmann (KR) configuration, where the incident light enters through the coupling glass prism, for these studies because the brightness of the system in RK configuration was satisfactory enough for all intensity measurements. Although the excitation is much stronger with the KR configuration, the precise observation angle-dependent measurements are more difficult. As we already observed,[22] there is no difference in θ_F in the two modes of excitation.

SPCE of QDs. We measured the fluorescence emission spectra of QDs observed in free space (FS, Figure 5, top) and through the hemispherical prism at the SPCE angle (Figure 5, bottom). The excitation was horizontally polarized. In the RK/FS mode, the vertical (V) and horizontal (H) emission intensities were similar. The difference in the emission intensity was only 23% between H and V; this indicates the low anisotropy of the studied system. In contrast, the SPCE (RK/SPCE mode) was highly polarized. This was shown by a large difference in the emission intensity of H vs V. The vertical emission signal was 95% less than the horizontal signal, which makes the V emission almost negligible. When the excitation light beam was rotated to the vertical position, the SPCE emission remained almost unchanged. These experiments showed the highly p-polarized property of QD SPCE.

Next, we measured the angular distribution of QD SPCE (Figure 6, top). The emission of the QDs on the SiO_2/Ag substrate was narrowly distributed around 48.5°, and the emission at this angle was several times stronger than that in free space (90−270°). To verify that this directional emission was due to SPCE, we used the TFCalc 3.5 program to theoretically predict the SPCE for a 25-nm-thick PVA surface. Figure 6, bottom, shows that the minimum reflectance angle of

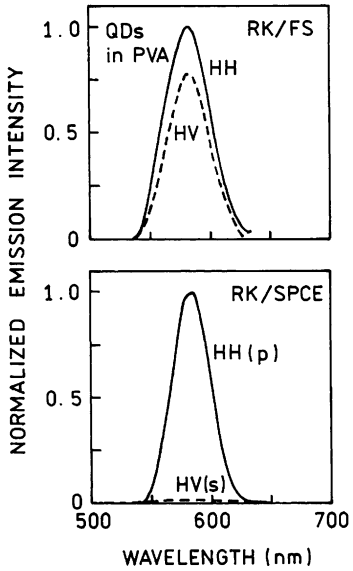

Figure 5. Emission spectra of PVA doped with quantum dots in free space (top) and at the SPCE angle of 48.5° (bottom). Whereas the free-space emission is weakly polarized, the SPCE is highly p-polarized (>95%).

585-nm incident light for a 25-nm-thick surface is 48.5°. This theoretical SPR angle is consistent with the experimentally measured QD SPCE angle.

We characterized the dependence of the fluorescence emission of the QDs versus observation angle. As shown in Figure 1, shorter-wavelength light entered the coupling prism at higher angles. The QD fluorescence spectrum shifted toward longer wavelengths when the observation angle decreased. A 6° difference in the observation angle was enough to shift the color emission from yellow (53°) to orange (47°) (Figure 7, top). Correspondingly, a shift of 13 nm in the fluorescence spectrum was observed when the angle was changed (Figure 7, bottom). This fluorescence shift did not occur when the fluorescence emission of the QDs (not interacting with metal surfaces or structures) was measured.

The fluorescence emission of QDs excited near the silver surface was photostable (Figure 8). We compared the photostabilities of QDs and rhodamine B (RhB) SPCEs. In these experiments, we prepared Ag/SiO_2 substrates and doped the 0.75% PVA with either QDs or RhB. The optical densities of RhB and the QDs were found to be roughly similar. However, the absorption of the QDs was low (about 0.005) and contained a scattering component. The number of photons absorbed by the QDs might be slightly lower than that absorbed by the rhodamine sample. Therefore, the zero-time intensities in Figure 8 are arbitrary and do not represent the quantum yield ratio. The power density for the photobleaching study was 2.0×10^5 W/m^2. The RhB SPCE intensity decreased quickly in time, with a half-life of 70 s, whereas the QDs fluorescence maintained bright emission. After 600 s, the emission of the QDs was unchanged, whereas the RhB signal decreased by 80%.

To verify that the fluorescence emission signals were indeed due to QDs and not to the PVA, we examined the emissions of three different surfaces: one without PVA, one with 0.75% PVA, and one with 0.75% PVA doped with QDs. Within the spectral region of 540−640 nm, there was no emission from surface without QDs, whereas the surface with QDs was bright. The estimated background signals from the surfaces without and with PVA and no QDs were below 1% of the fluorescence signal observed from the sample with QDs.

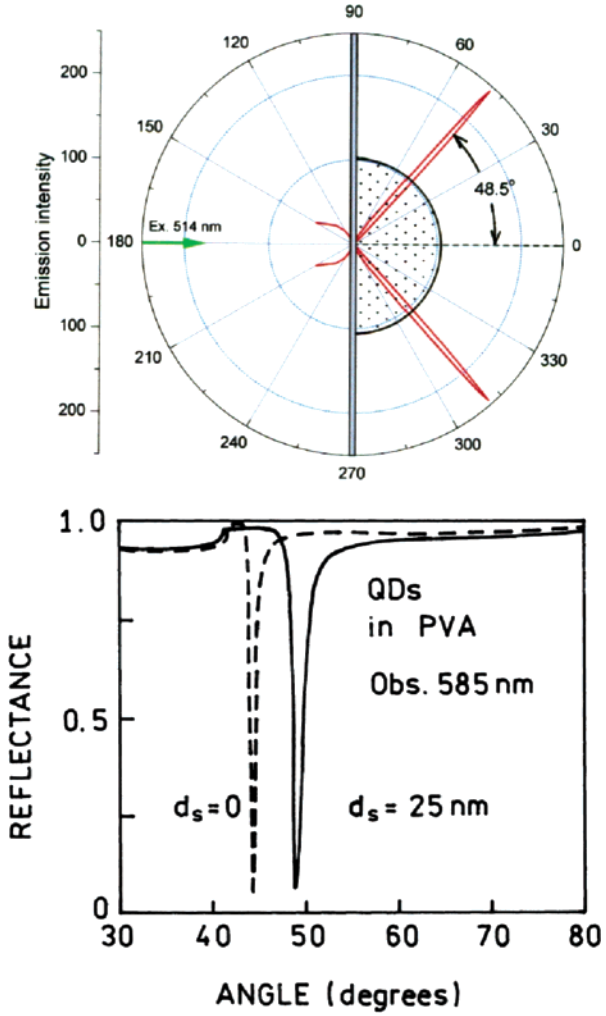

Figure 6. Angular distribution of QD SPCE (top). The radiation is narrowly distributed around 48.5°. At this direction, the intensity is several times stronger than in free space (90°−270°). The calculated reflectivity profile for a five-phase system (Figure 1) is shown in the bottom panel. The minimum reflectivity at 48.5° corresponds to the sample thickness of 25 nm.

Interestingly, we also observed another phenomenon. The excitation radiation (514 nm) from the assembled substrate containing QDs was visually stronger than that from assembled substrates without QDs. Figure 9 shows the integrated intensities of a 514-nm light source for the substrates with no PVA, with PVA but no QDs, and with PVA doped with QDs to be 10:16:85. Although we do not know the exact mechanism for this enhancement, we suspect that the QDs might assist in the coupling of scattered light to surface plasmons. Kume et al. obtained similar results.[30] They showed that the addition of metal particles to a dielectric layer near thin metal mirror increased the intensity of the illuminating source.

Also, a very slight difference between the SPCE angles observed for PVA-only and QD-doped PVA films (middle and lower panels in Figure 9) suggests that the presence of QDs does not significantly change the refractive index of PVA sample.

The results show that QDs coated on a Ag/SiO_2 substrate have fluorescence emissions that are directional and highly polarized. These properties are not common with QDs sputtered on glass surfaces without the Ag/SiO_2. These results strongly suggest that QD emissions are due to surface-plasmon coupling.

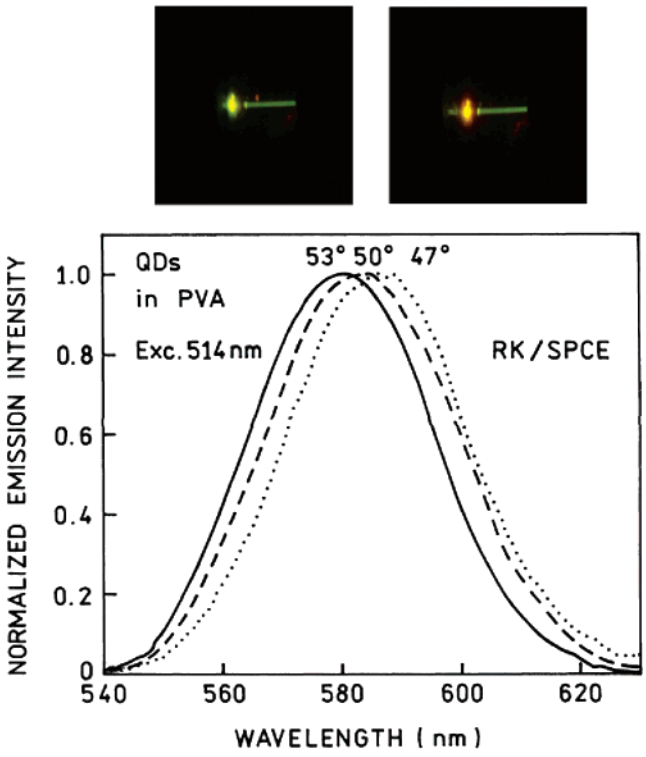

Figure 7. Observation-angle-dependent spectra of QD SPCE. The top panel shows the photographs for 53° (left) and 47° (right) taken from a distance of about 3 m.

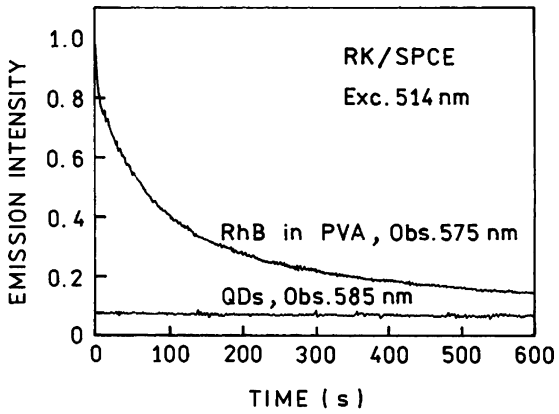

Figure 8. Photostability tests for SPCE of QDs and RhB. During the entire 10-min exposure to the intense (100-mW, 0.7-mm-diameter) 514-nm excitation, the emission intensity of the QD SPCE did not change.

Conclusions

In this article, we demonstrated and measured the surface-plasmon-coupled emission of high-quality QDs. As a result, QDs coupled to nanometer-sized metallic substrates emit light in a polarized and directional fashion. Uncoupled QDs do not have these properties. All other properties of QDs are similar between SPC and non-SPC emission.

These findings might have implications in numerous applications. The multiplexing capability and sensitivity of surface plasmon resonance detection systems can be dramatically improved using QDs as probes. The surface plasmon excitation of QDs on the Ag/SiO_2 surface will occur only near the metal surface (~150 nm). Autofluorescence beyond the 150-nm range will be rejected, and this can lead to a better signal-to-noise ratio and, therefore, better detection sensitivity. We believe that the detection limit with the SPCE technique will be superior to that with free-space observation, especially for samples with

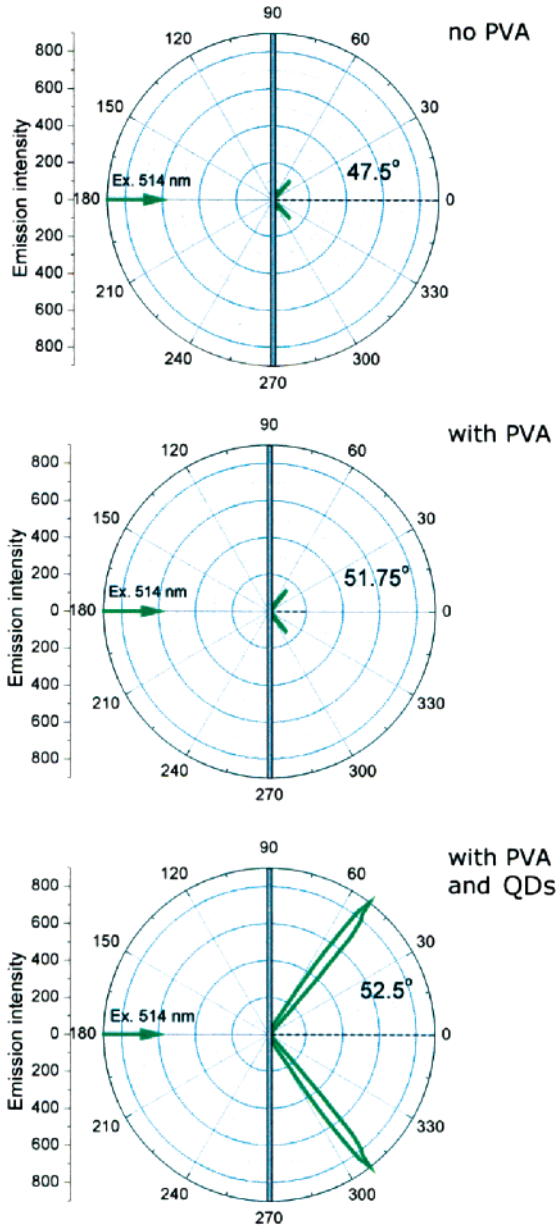

Figure 9. Angular distribution of 514-nm excitation transformed to a polarized directional radiation of the same wavelength. Essentially, the surface plasmons cannot be excited in the RK configuration by the incident light beam from the air. Observed cones of 514-nm radiation are due to the imperfections of the sample layer (roughness). Whereas the PVA itself does not introduce any significant roughness (compare top and middle panels), the presence of QDs causes a many-fold increase in the 514-nm directional radiation.

thicknesses lower than 150 nm. The collection efficiency of directional rather than isotropic emission can be improved easily in spectroscopic and microscopic (TIRF format) measurements. In our experiment, we collected through the fiber only about 0.5% of the hollow cone emission (Figure 1). The tunable emission and monochromatic excitation wavelength of the QDs will extend surface plasmon detection techniques to detect more than one or two biomolecules at a time while the improved photostability will extend the time permitted for studying biomolecule interactions. Finally, the polarization properties of QD SPCE can be exploited for drug-discovery applications given that this analytical mode is one of the most common approaches for analyzing drug to target interactions.

Beyond the development of QD SPCE bioassays, it would be interesting to study QD coupling to metallic nanostructures.

Metallic nanostructures have tunable surface plasmon resonances, and the coupling of QDs to such structures might yield the discovery of interesting optical and electronic properties. This might also lead to applications in biological detection, optical coatings, and nanoelectronics.

Acknowledgment. This work was supported by NIH, National Center for Research Resources, RR-08119. W.J. acknowledges Ontario Graduate Scholarship for financial support. W.C.W.C. acknowledges NSERC, CFI, OIT, and University of Toronto (Start-up) for financial support.

References and Notes

(1) Zhong, X.; Feng, Y.; Knoll, W.; Han, M. Alloyed $Zn_xCd_{1-x}S$ nanocrystals with highly narrow luminescence spectral width. *J. Am. Chem. Soc.* **2003**, *125*, 13559−13563.

(2) Qu, L.; Peng, Z. A.; Peng, X. Alternative routes toward high quality CdSe nanocrystals. *Nano Lett.* **2001**, *1* (6), 333−337.

(3) Peng, X.; Manna, L.; Yang, W.; Wickham, J.; Scher, E.; Kadavanich, A.; Alivisatos, A. P. Shape control of CdSe nanocrystals. *Nature* **2000**, *404*, 59−61.

(4) Murray, C. B.; Norris, D. J.; Bawendi, M. G. Synthesis and characterization of nearly monodisperse CdE (E = S, Se, Te) semiconductor nanocrystallites. *J. Am. Chem. Soc.* **1993**, *115*, 8706−8715.

(5) Hines, M. A.; Guyot-Sionnest, P. Synthesis and characterization of strongly luminescing ZnS-capped CdSe nanocrystals. *J. Phys. Chem. B* **1996**, *100*, 468−471.

(6) Schultz, S.; Smith, D. R.; Mock, J. J.; Schultz, D. A. Single-target molecule detection with nonbleaching multicolor optical immunolabels. *Proc. Natl. Acad. Sci.* **2000**, *97* (3), 996−1001.

(7) Han, M.; Gao, X.; Su, J. Z.; Nie, S. Quantum-dot-tagged microbeads for multiplexed optical coding of biomolecules. *Nat. Biotechnol.* **2001**, *19*, 631−635.

(8) Chan, W. C. W.; Maxwell, D. J.; Gao, X. H.; Bailey, R. E.; Han, M. Y.; Nie, S. M. Luminescent quantum dots for multiplexed biological detection and imaging. *Curr. Opin. Biotechnol.* **2002**, *13*, 40−46.

(9) Chan, W. C. W.; Nie, S. Quantum dot bioconjugates for ultrasensitive nonisotopic detection. *Science* **1998**, *281* (5385), 2016−2018.

(10) Dubertret, B.; Skourides, P.; Norris, D. J.; Noireaux, V.; Brivanlou, A. H.; Libchaber, A. In vivo imaging of quantum dots encapsulated in phospholipid micelles. *Science* **2002**, *298*, 1759−1762.

(11) Cao, Y. C.; Jin, R.; Mirkin, C. A. Nanoparticles with Raman spectroscopic fingerprints for DNA and RNA detection. *Science* **2002**, *297*, 1536−1539.

(12) Raether, H. Surface plasma oscillations and their applications. In *Physics of Thin Films, Advances in Research and Development*; Hass, G., Francombe, M. H., Hoffman, R. W., Eds.; Academic Press: New York, 1977; Vol. 9, pp 145−261.

(13) Pockrand, I. Surface plasma oscillations at silver surfaces with thin transparent and absorbing coatings. *Surf. Sci.* **1978**, *72*, 577−588.

(14) Nelson, B. P.; Frutos, A. G.; Brockman, J. M.; Corn, R. M. Near-infrared surface plasmon resonance measurements of ultrathin films. 1. Angle shift and SPR imaging experiments. *Anal. Chem.* **1999**, *71*, 3928−3934.

(15) Liedberg, B.; Lundstrom, I. Principles of biosensing with an extended coupling matrix and surface plasmon resonance. *Sens. Actuators B* **1993**, *11*, 63−72.

(16) Frey, B. L.; Jordan, C. E.; Kornguth, S.; Corn, R. M. Control of the specific adsorption of proteins onto gold surface with poly(L-lysine) monolayers. *Anal. Chem.* **1995**, *67*, 4452−4457.

(17) Salamon, Z.; Macleod, H. A.; Tollin, G. Surface plasmon resonance spectroscopy as a tool for investigating the biochemical and biophysical properties of membrane protein systems. I: Theoretical principles. *Biochim. Biophys. Acta* **1997**, *1331*, 117−129.

(18) Peterlinz, K. A.; Georgiadis, R. In situ kinetics of self-assembly by surface plasmon resonance spectroscopy. *Langmuir* **1996**, *12*, 4731−4740.

(19) Yu, F.; Yao, D.; Knoll, W. Surface plasmon field-enhanced fluorescence spectroscopy studies of the interaction between an antibody and its surface-coupled antigen. *Anal. Chem.* **2003**, *75*, 2610−2617.

(20) Ekgasit, S.; Thammacharoen, C.; Knoll, W. Surface plasmon resonance spectroscopy based on evanescent field treatment. *Anal. Chem.* **2004**, *76*, 561−568.

(21) Lakowicz, J. R. Radiative decay engineering 3. Surface plasmon-coupled directional emission. *Anal. Biochem.* **2004**, *324*, 153−169.

(22) Gryczynski, I.; Malicka, J.; Gryczynski, Z.; Lakowicz, J. R. Radiative decay engineering 4. Experimental studies of surface plasmon-coupled directional emission. *Anal. Biochem.* **2004**, *324*, 170−182.

(23) Malicka, J.; Gryczynski, I.; Gryczynski, Z.; Lakowicz, J. R. Use of surface plasmon-coupled emission to measure DNA hybridization. *J. Biomol. Screening* **2004**, *9* (3), 208−215.

(24) Matveeva, E.; Malicka, J.; Gryczynski, I.; Gryczynski, Z.; Lakowicz, J. R. Multiwavelength immunoassays using surface plasmon-coupled emission. *Biochem. Biophys. Res. Commun.* **2004**, *313*, 721−726.

(25) Gryczynski, I.; Malicka, J.; Gryczynski, Z.; Lakowicz, J. R. Surface plasmon-coupled emission using gold films. *J. Phys. Chem. B* **2004**, *108*, 12568−12574.

(26) Bruchez, M., Jr.; Maronne, M.; Gin, P.; Weiss, S.; Alivisatos, S. P. Semiconductor nanocrystals as fluorescent biological labels. *Science* **1998**, *281* (5385), 2013−2016.

(27) Mattoussi, H.; Mauro, J. M.; Goldman, E. R.; Green, T. M.; Anderson, G. P.; Sundar, V. C.; Bawendi, M. B. Bioconjugation of highly luminescent colloidal CdSe−ZnS quantum dots with an engineered two-domain recombinant protein. *Phys. Status Solidi B* **2001**, *244* (1), 277−283.

(28) Akerman, M. E.; Chan, W. C. W.; Laakkonen, C.; Bhatia, S. N.; Ruoslahti, E. Nanocrystal targeting *in vivo*. *Proc. Nat. Acad. Sci.* **2002**, *99* (20), 12617−12621.

(29) Jiang, W.; Mardyani, S.; Fischer, H.; Chan, W. C. W. Large-scale surface modification of TOPO-coated quantum dots for biological applications, manuscript submitted.

(30) Kume, T.; Hayashi, S.; Yamamoto, K. A new method of surface plasmon excitation using metallic fine particles. *Mater. Sci. Eng.* **1996**, *A217/218*, 171−175.